Chaos in small networks of theta neurons

Carlo R. Laing*
Institute of Natural and Mathematical Sciences, Massey University, Private Bag 102-904 NSMC, Auckland, New Zealand. phone: +64-9-414 0800 extn. 43512 fax: +64-9-443 9790
(Dated: June 25, 2018)

We consider small networks of instantaneously coupled theta neurons. For inhibitory coupling and fixed parameter values some initial condition give chaotic solutions while others give quasiperiodic ones. This behaviour seems to result from the reversibility of the equations governing the networks' dynamics. We investigate the robustness of the chaotic behaviour with respect to changes in initial conditions and parameters, and find the behaviour to be quite robust, as long as the reversibility of the system is preserved.

PACS numbers: 05.45.Ac , 05.45.Xt, 87.19.ll, 87.19.lj, 87.19.lm
Keywords: theta neuron, chaos, reversibility

The behaviour of large networks of model neurons is often of interest, but sometimes small networks provide a better description of the biological system of interest. Surprisingly, very small networks of theta neurons (describing the normal form of a saddle-node on invariant circle bifurcation) can show chaotic behaviour. Chaotic solutions coexist with quasiperiodic ones, apparently as a result of the reversibility of system's dynamics. This behaviour is quite robust to changes in parameters, and to making the neurons non-identical.

I. INTRODUCTION

Studies of networks of neurons often consider large networks of heterogeneous neurons, under the assumptions that the behaviour of an individual neuron cannot be significant, and that real neurons are not identical [1–3]. However, in some circumstances small networks are of interest [4, 5], and the special case of identical neurons allows one to use techniques from the study of symmetric dynamical systems [6–8]. In a recent paper [9] we considered large (sometimes infinite) networks of all-to-all coupled identical theta neurons. These networks are unusual in that there exists an exact method for reducing the dimensionality of the system from N (the number of neurons in the network) to 3 using the Watanabe/Strogatz ansatz [10, 11]. One interesting aspect of the dynamics of these systems is that for instantaneous inhibitory coupling the dynamics appears chaotic for some initial conditions, but quasiperiodic for other initial conditions. In this paper we undertake a more thorough investigation into this behaviour, determining how robust this chaotic behaviour is to changes in parameters and initial conditions.

We now briefly survey some relevant previous work. The notion of chaotic behavior has been around for a number of decades, and chaotic attractors in symmetric systems of coupled oscillators were investigated by a number of researchers. For example, [12] investigated networks of 3 or 4 symmetrically-coupled forced identical oscillators. These oscillators were implemented using analogue electrical circuits and chaotic attractors with varing degrees of symmetry were observed. A particularly simple class of oscillator is the phase oscillator, where the state of each oscillator is described by a single angular variable. These are often appropriate models for networks of weakly coupled oscillators [6, 13]. Kuramoto-type networks, in which phase oscillators are coupled through a sinusoidal function of phase differences, have been well-studied [14, 15]. The question as to whether this type of network can have chaotic solutions has been addressed by several groups. [16] considered small networks of identical, all-to-all coupled phase oscillator networks and found that four or more oscillators were required, along with two or more harmonics in the coupling function. [17] found chaotic behaviour in networks of four or more heterogeneous phase oscillators coupled with just a single harmonic in their coupling function. Extensions to networks of phase oscillators with nonpairwise interactions also found chaotic behavior [18]. Chaos has been found in networks comprised of two symmetric subnetworks, with different coupling within and between subnetworks [19, 20], and in Kuramoto oscillators on a ring [21, 22].

All of the studies mentioned above considered networks in which coupling was through *phase differences*, with the consequence that only differences in frequencies between oscillators, not their absolute frequencies, can be considered

*Electronic address: c.r.laing@massey.ac.nz

meaningful. In contrast theta neurons, studied here, can fire at arbitrarily high frequencies, or not at all, depending on their input [23, 24]. Also, they are coupled through functions of phase, not phase differences. The only studies of chaos in networks of theta neurons we are aware of are [9, 25, 26] and [27], which actually considered quadratic integrate-and-fire neurons, equivalent under a coordinate tranformation to theta neurons. In [25] the authors considered large sparse networks of theta neurons, coupled through delta function current pulses. [26] generated chaos in large or infinite networks by periodically varying the input current to each neuron, making the system nonautonomous. In [27] the authors consider large networks with delayed inhibition, whereas here we concentrate on small networks with instantanous inhibitory coupling. Also note that several groups [28–30] have observed irregular behaviour in large networks of integrate-and-fire neurons with delayed inhibitory coupling. However, the only study of small networks appears to be [9].

We consider small networks of all-to-all coupled theta neurons. The theta neuron is the canonical model for a Type I neuron for which the onset of firing is through a saddle-node on an invariant circle bifurcation [23, 24]. It can be derived by a nonlinear coordinate transformation from the quadratic integrate-and-fire neuron model [31]. The equations of the network are

$$\frac{d\theta_i}{dt} = 1 - \cos\theta_i + (1+\cos\theta_i)(\eta + \kappa I) \tag{1}$$

for $i = 1, 2, \ldots N$, where η and κ are constants and

$$I = \frac{a_n}{N}\sum_{i=1}^{N}(1-\cos\theta_i)^n \tag{2}$$

where a_n is chosen so that

$$\int_0^{2\pi} a_n(1-\cos\theta)^n \; d\theta = 2\pi \tag{3}$$

i.e. $a_n = 2^n(n!)^2/(2n)!$. The function $a_n(1-\cos\theta_i)^n$ is meant to mimic the action potential produced when neuron i fires, i.e. θ_i increases through π. Such models have been studied in the limit of $N \to \infty$ and with randomly chosen η's for each neuron by [26, 32]. An important observation is that this system is reversible under the transformation $(t, \{\theta_i\}) \mapsto (-t, \{-\theta_i\})$ for all i.

II. RESULTS FOR NETWORKS OF 3 NEURONS

For some parameters the system (1)-(2) with $N = 3$ can show chaotic behaviour, as seen in Fig. 1(a). However, for the same parameter values different initial conditions can result in quasiperiodic behaviour instead, as in Fig. 1(b). Such a mixture of chaotic and more regular behaviour has been previously observed in several other reversible systems [33, 34].

In order to better understand this behaviour we first consider a sweep through all initial conditions. Setting $\theta_1(0) = 0$ and varying $\theta_2(0)$ and $\theta_3(0)$ we obtain Fig. 2. We see two different regions, one in which solutions are apparently quasiperiodic with maximal Lyapunov exponent equal to zero, and another in which solutions are chaotic (i.e. have positive maximal Lyapunov exponent). Note that the figure is symmetric about the diagonal, and on the diagonal the resulting solutions cannot be chaotic, as the system is then two-dimensional [1].

To visualise the solutions we put a Poincaré section at $\theta_1 = \pi$, $d\theta_1/dt > 0$, with results shown in Fig. 3. Since the neurons are identical, their firing order must be preserved. In this case, the initial conditions were ordered $0 = \theta_1(0) < \theta_2(0) < \theta_3(0) < 2\pi$, and this is why points only appear in three sectors in Fig. 3. We see evidence of some chaotic solutions and two regions corresponding to quasiperiodic solutions in the upper right and lower left sectors. Quasiperiodic solutions alternate between these two regions, so that when $\theta_1 = \pi$, then, say, $\pi < \theta_2 < \theta_3 < 2\pi$ (upper right sector), while the next time $\theta_1 = \pi$, we will have $0 < \theta_2 < \theta_3 < \pi$ (lower left sector). At the centre of the quasiperiodic orbits is a periodic one which repeats after each phase has increased through 4π, shown in Fig. 4. On this orbit each neuron takes a turn being inhibited (θ decreases) while the other two fire: firstly neuron 2, then neuron 3 and finally neuron 1. (There is of course a solution with the opposite ordering.) While different initial conditions

[1] All computations have been performed in Matlab with integrator ode113 using absolute tolerance of 10^{-10} and relative tolerance of 10^{-8}. Jacobians needed for Lyapunov exponent calculations are found analytically.

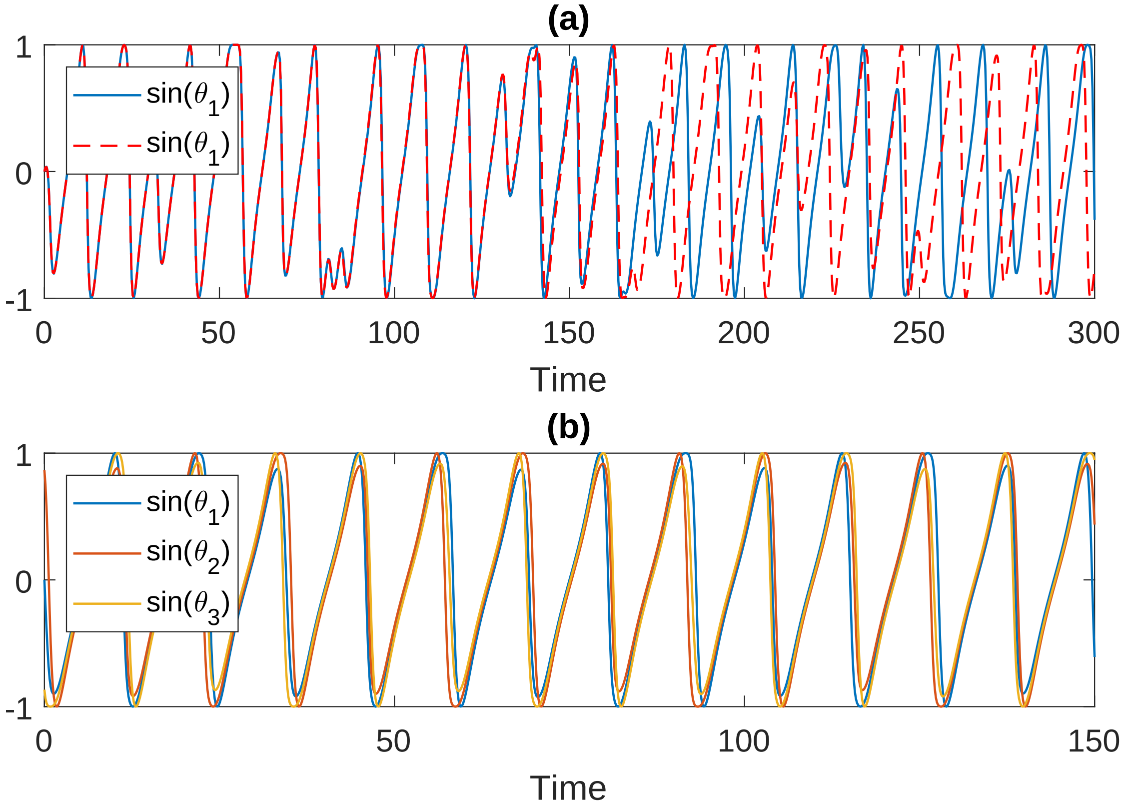

Figure 1: (a) $\sin(\theta_1)$ for initial conditions $(\theta_1, \theta_2, \theta_3) = (0, 1, 6)$ (red dashed) and $(10^{-4}, 1, 6)$ (blue solid). This shows the exponential divergence characteristic of a chaotic solution. (b) $\sin(\theta_i)$ for $i = 1, 2, 3$ with initial conditions $(\theta_1, \theta_2, \theta_3) = (0, 2\pi/3, 4\pi/3)$. This is a quasiperiodic solution. Parameters: $N = 3, n = 2, \kappa = -0.75, \eta = 0.1$.

are needed to observe different quasiperiodic orbits, an initial condition in the chaotic region seems to fully explore this region.

Full synchrony corresponds to the central point in Fig. 3, while on the diagonal and the lines $\theta_2 = \pi$ and $\theta_3 = \pi$ two of the three oscillators are synchronised. To linear order, the fully synchronous state is found to be neutrally stable. Defining $x \equiv \theta_2 - \pi$ and $y \equiv \theta_3 - \pi$ and only plotting points with $\sqrt{x^2 + y^2} < 0.1$ from a simulation of length 10^5 time units we obtain Fig. 5(a). Assuming that these points are generated by the second order map

$$\begin{pmatrix} x_{n+1} \\ y_{n+1} \end{pmatrix} = \begin{pmatrix} a_1 & a_2 \\ b_1 & b_2 \end{pmatrix} \begin{pmatrix} x_n \\ y_n \end{pmatrix} + \begin{pmatrix} a_{11}x_n^2 + a_{12}x_n y_n + a_{22}y_n^2 \\ b_{11}x_n^2 + b_{12}x_n y_n + b_{22}y_n^2 \end{pmatrix} \tag{4}$$

and using nonlinear least squares to find the coefficients which best fit all of the points in Fig. 5(a) we obtain the map

$$\begin{pmatrix} x_{n+1} \\ y_{n+1} \end{pmatrix} = \begin{pmatrix} 0.999 & 0 \\ 0 & 0.999 \end{pmatrix} \begin{pmatrix} x_n \\ y_n \end{pmatrix} + \begin{pmatrix} 0.376x_n^2 - 0.773x_n y_n + 0.011y_n^2 \\ -0.009x_n^2 - 0.743x_n y_n + 0.377y_n^2 \end{pmatrix} \tag{5}$$

(coefficients rounded to 3 decimal places). The direction field induced by this map is shown in Fig. 5(b). Note that the x and y axes, as well as the diagonal, are all approximately invariant.

An interesting aspect of this system involves the amount of time spent within a given distance of the synchronous state (the origin). Assuming that the dynamics of the map (5) are close to those of

$$\begin{pmatrix} x_{n+1} \\ y_{n+1} \end{pmatrix} = \begin{pmatrix} x_n \\ y_n \end{pmatrix} + \begin{pmatrix} ax_n^2 - bx_n y_n \\ -bx_n y_n + ay_n^2 \end{pmatrix} \tag{6}$$

for some positive constants a, b, consider the initial condition $(x_0, y_0) = (\epsilon, -\epsilon); 0 < \epsilon \ll 1$. The y_n decay to zero from below, so the x dynamics are approximately $x_{n+1} = x_n + ax_n^2$. Since the x_n change slowly over time we can approximate this map by the differential equation $dx/dt = ax^2$ with $x(0) = \epsilon$. The time for x to reach a significant positive value then scales as ϵ^{-1}. This is in contrast with a hyperbolic saddle governed by, say, $dx/dt = \lambda x; dy/dt = -\mu y$ for some positive λ, μ. Solving the x dynamics with $x(0) = \epsilon$ gives an escape time scaling of $-\ln \epsilon$.

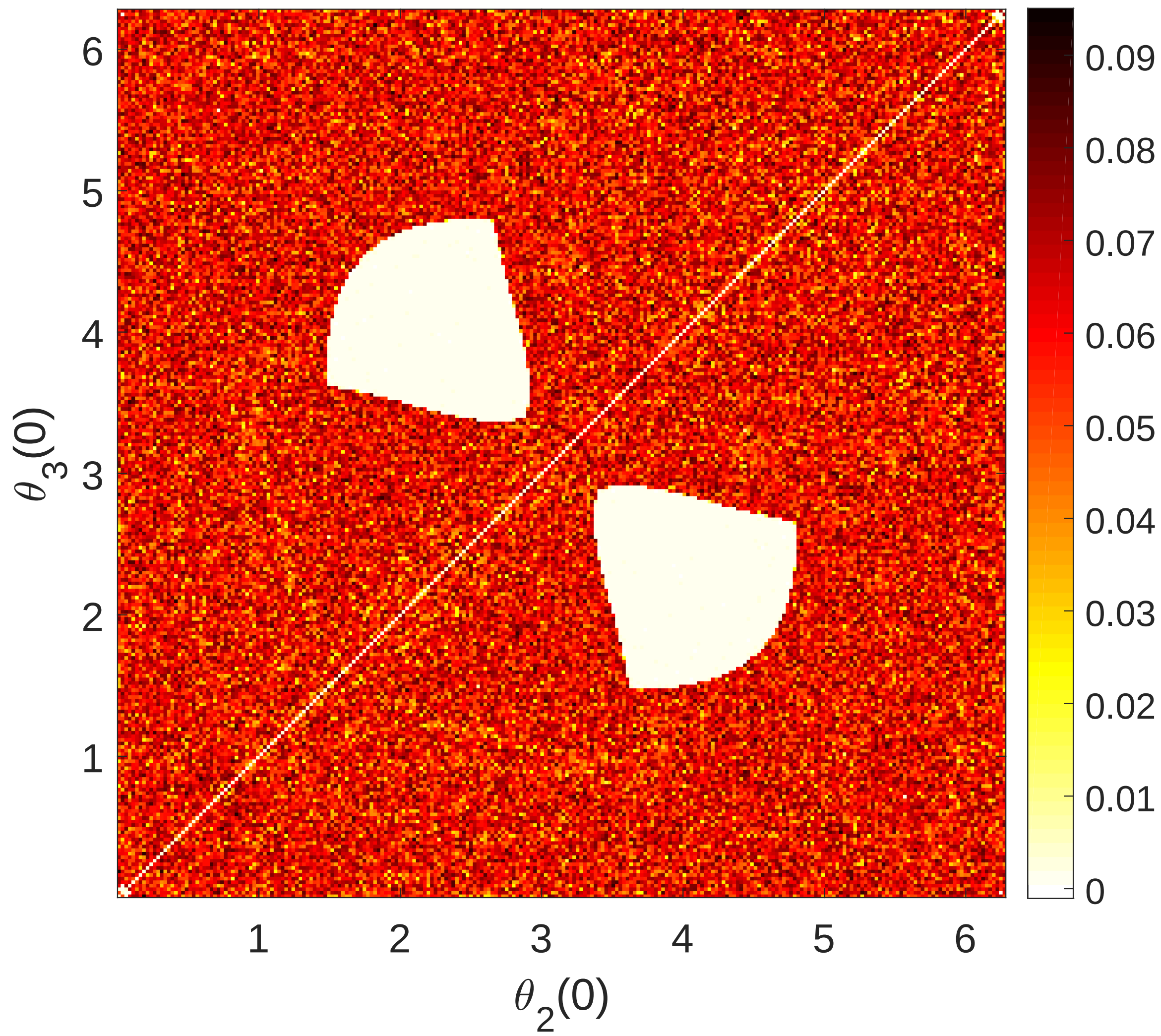

Figure 2: Maximal Lyapunov exponent for solutions starting with $\theta_1(0) = 0$ and $\theta_2(0)$ and $\theta_3(0)$ given by the values shown. Most initial conditions result in chaotic solutions (positive Lyapunov exponent) while some give quasiperiodic solutions (zero Lyapunov exponent). Parameters: $N = 3, n = 2, \kappa = -0.75, \eta = 0.1$.

We now consider varying other parameters. Sweeping through κ and $\theta_3(0)$ for fixed $\eta, \theta_1(0)$ and $\theta_2(0)$ we obtain Fig. 6. We see that a wide range of initial conditions and values of κ result in chaotic behaviour, and also that if κ is too large and negative, or too close to zero, the motion is not chaotic (at least for these initial conditions). The abrupt transition from chaotic behaviour for large negative κ results from the existence of a stable fixed point for these values of κ. If κ is small the neurons are weakly coupled. Thus the theory of weakly coupled oscillators is applicable [6, 13, 35] and the system can be reduced to a pair of equations involving only phase differences. The dynamics will lie on a two-torus and chaotic dynamics will be impossible. Simulations with positive κ and randomly chosen initial conditions (not shown) never found chaotic behaviour, consistent with the results in [9].

Sweeping through η and $\theta_3(0)$ for fixed $\kappa, \theta_1(0)$ and $\theta_2(0)$ we obtain Fig. 7. We also see that a wide range of initial conditions and values of η result in chaotic behaviour, and also that if η is too large, the motion is not chaotic (at least for these initial conditions). Varying n and $\theta_3(0)$ we obtain Fig. 8. Solutions are not chaotic for $n = 1$ and the maximal exponent seems to rise with n until about $n = 10$ after which is decreases, as does the proportion of values of $\theta_3(0)$ leading to chaotic behaviour.

In the limit $n \to \infty$, (2) becomes

$$I = \frac{2\pi}{N} \sum_{i=1}^{N} \delta(\theta_i - \pi) \tag{7}$$

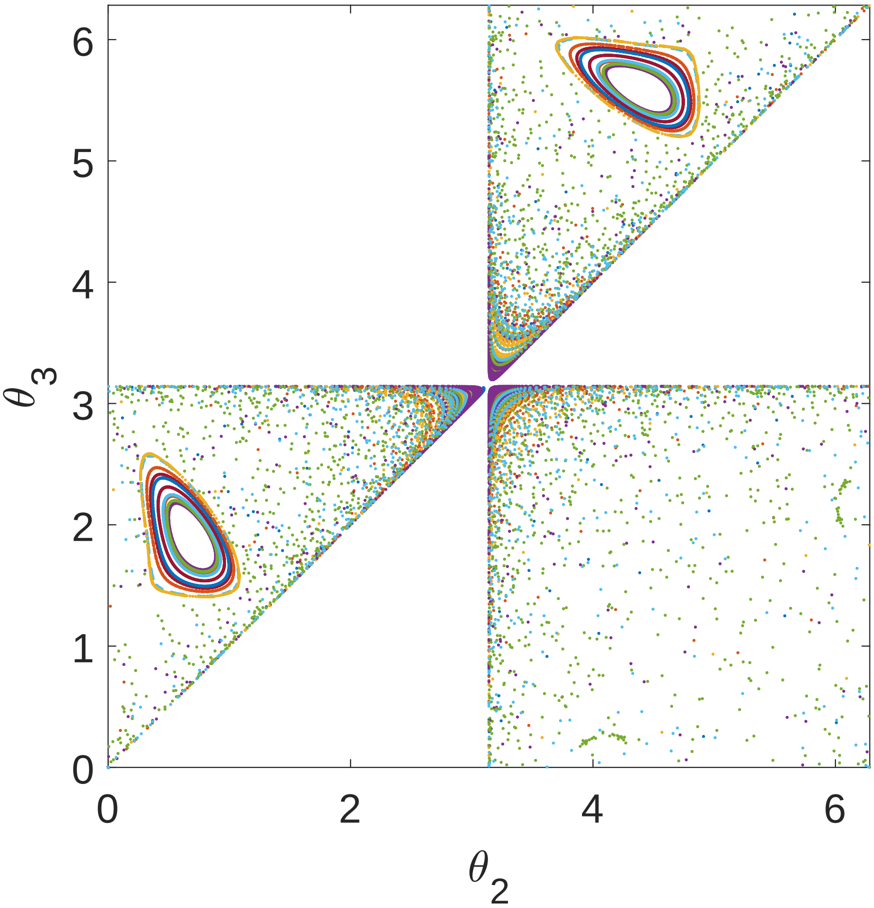

Figure 3: Poincaré section at $\theta_1 = \pi$ with $d\theta_1/dt > 0$. 20 different initial conditions were used and each solution starting with a specific initial condition is plotted a different colour. We see coexisting chaotic and quasiperiodic solutions. Parameters: $N = 3, n = 2, \kappa = -0.75, \eta = 0.1$.

where δ is the Dirac delta function. If t_j^k is the kth firing time of neuron j then we have [25]

$$I = \frac{\pi}{N} \sum_{j=1}^{N} \sum_{k} \delta(t - t_j^k) \tag{8}$$

where the sum over k is only over past firing times. We can calculate the maximal Lyapunov exponent for this network as shown in the appendix, and we find that the exponent is zero for all initial conditions. This dichotomy of chaotic solutions for networks of neurons which interact in a smooth way versus nonchaotic dynamics in networks with instantaneous interactions has been previously remarked upon [25].

Now consider the case where the neurons are nonidentical but the system is still reversible. To do this we replace (1) by

$$\frac{d\theta_i}{dt} = 1 - \cos\theta_i + (1 + \cos\theta_i)(\eta_i + \kappa I) \tag{9}$$

fix $\eta_1 = 0.1$ and vary η_2 and η_3. Doing so we obtain Fig. 9. We see that the chaotic behaviour persists as these parameters are varied, but not in a simple way.

One concern is that self-coupling may be unrealistic and the cause of the chaotic behaviour. Removing the self-coupling we obtain

$$\frac{d\theta_i}{dt} = 1 - \cos\theta_i + (1 + \cos\theta_i)(\eta + \kappa I_i) \tag{10}$$

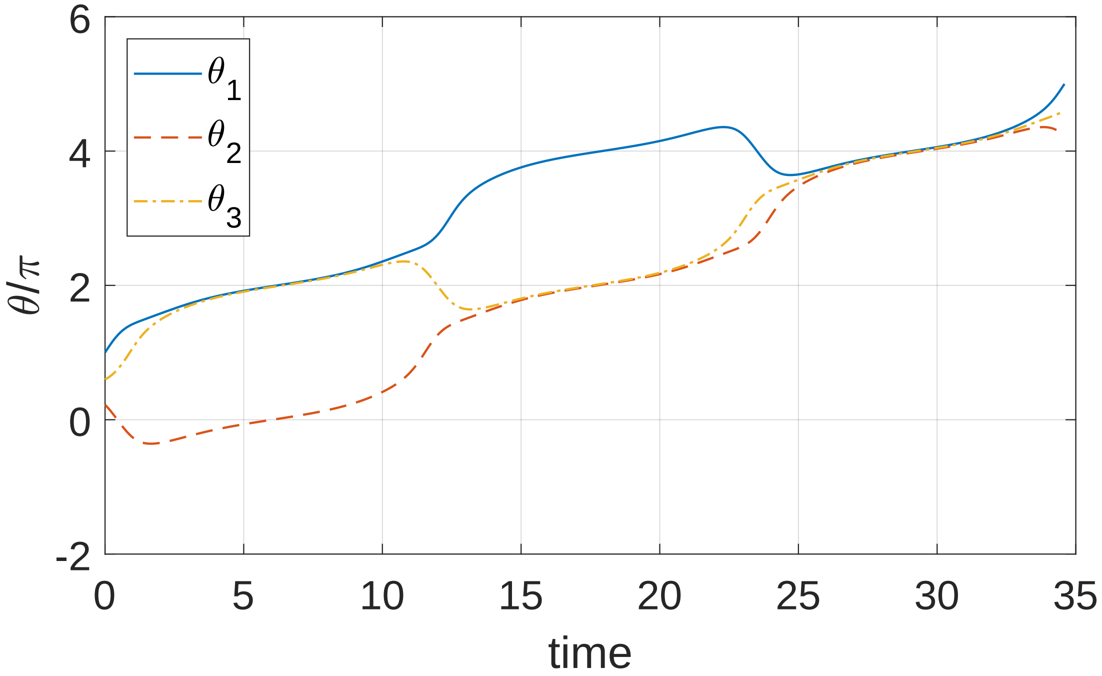

Figure 4: One period of the periodic orbit at the centre of the quasiperiodic regions in Fig. 3. Initially $\theta_1 = \pi$ and at the final time $\theta_1 = 5\pi$. Parameters: $N = 3, n = 2, \kappa = -0.75, \eta = 0.1$.

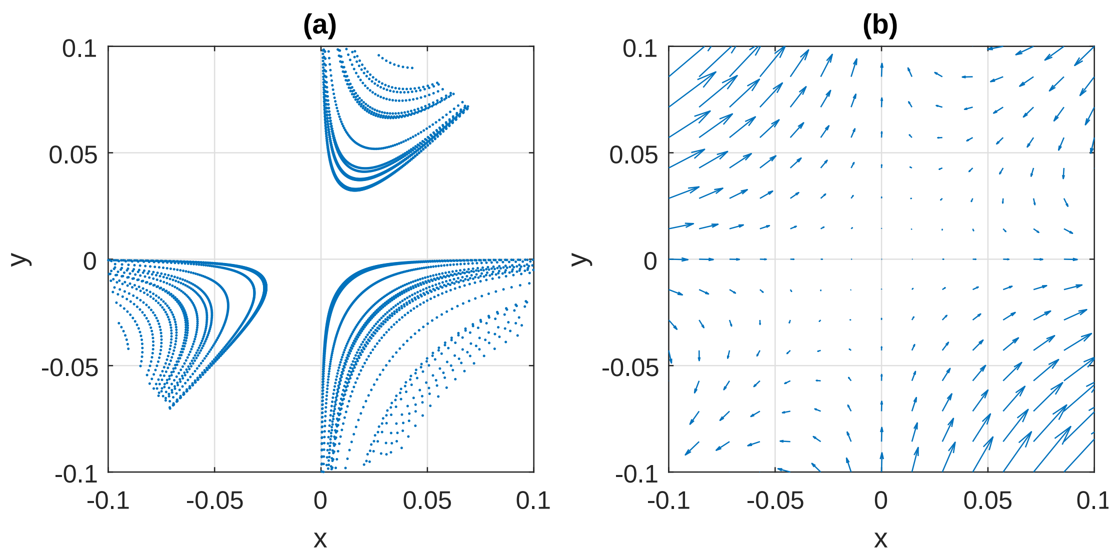

Figure 5: (a) points from the Poincaré section $\theta_1 = \pi$ with $d\theta_1/dt > 0$ with $\sqrt{x^2+y^2} < 0.1$, i.e. in a neighbourhood of the fully synchronous state. (b) Direction field induced by the map (5), obtained by fitting a general second-order map to the points in panel (a). Parameters: $N = 3, n = 2, \kappa = -0.75, \eta = 0.1$.

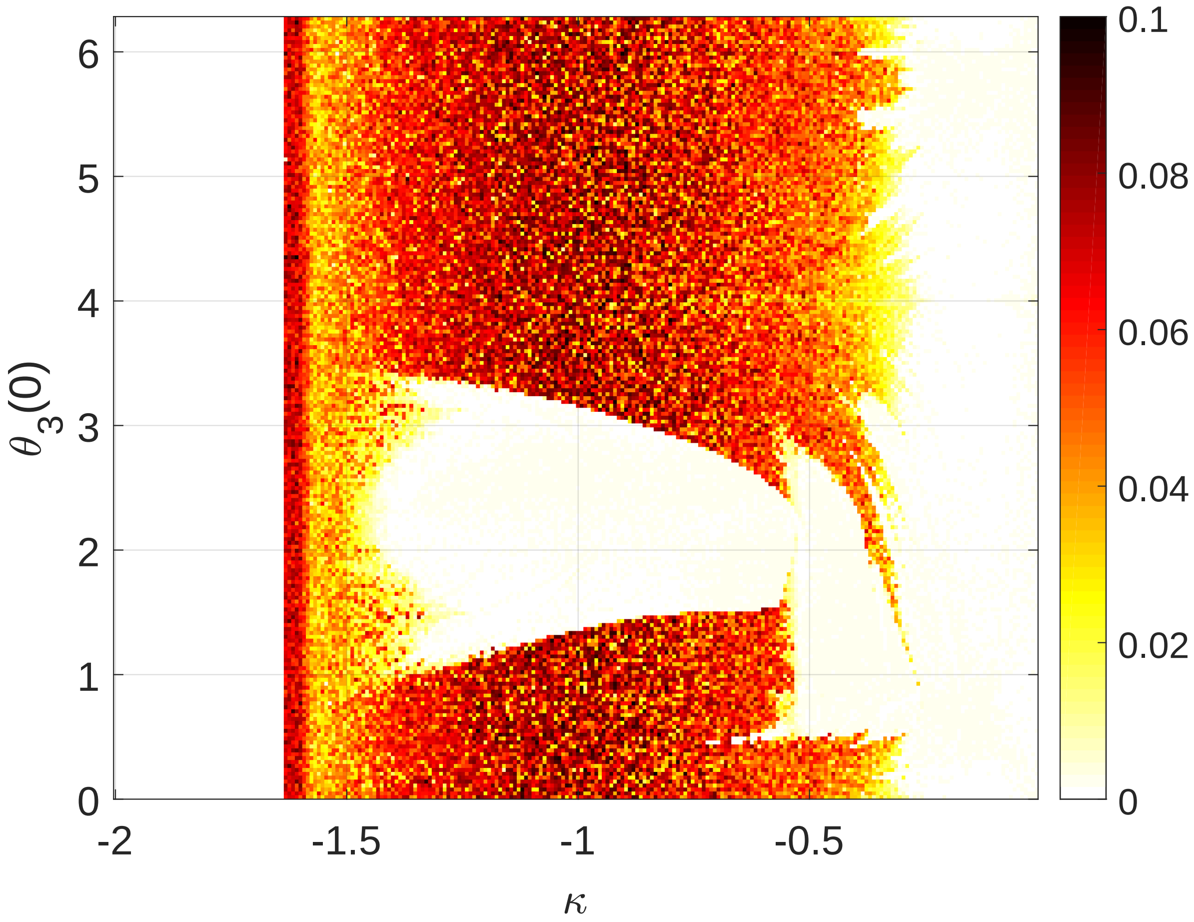

Figure 6: Maximal Lyapunov exponent for solutions starting with $\theta_1(0) = 0$, $\theta_2(0) = 4$ and $\theta_3(0)$ given by the value shown. Chaotic solutions have positive Lyapunov exponent. Parameters: $N = 3, n = 2, \eta = 0.1$.

for $i = 1, 2, 3$, where

$$I_i = \frac{a_n}{2} \sum_{\substack{j=1 \\ j \neq i}}^{3} (1 - \cos\theta_j)^n \tag{11}$$

and a_n is as in (3). Studying the network (10)-(11), we see from Fig. 10 that even without self-coupling the network can be chaotic for a range of initial conditions.

We also considered a mix of inhibitory and excitatory neurons, modifying (1) to

$$\frac{d\theta_i}{dt} = 1 - \cos\theta_i + (1 + \cos\theta_i)(\eta + I); \qquad i = 1, 2, 3 \tag{12}$$

where

$$I = a_n \left[-0.75(1 - \cos\theta_1)^n - 0.75(1 - \cos\theta_2)^n + k(1 - \cos\theta_3)^n \right] / N \tag{13}$$

so that neurons 1 and 2 are inhibitory and neuron 3 is inhibitory if $k < 0$ and excitatory if $k > 0$. Setting $\eta = 0.2$ and $n = 2$ and randomly choosing initial conditions, we found chaotic solutions for $k < 0$ but none for $k > 0$ (not shown).

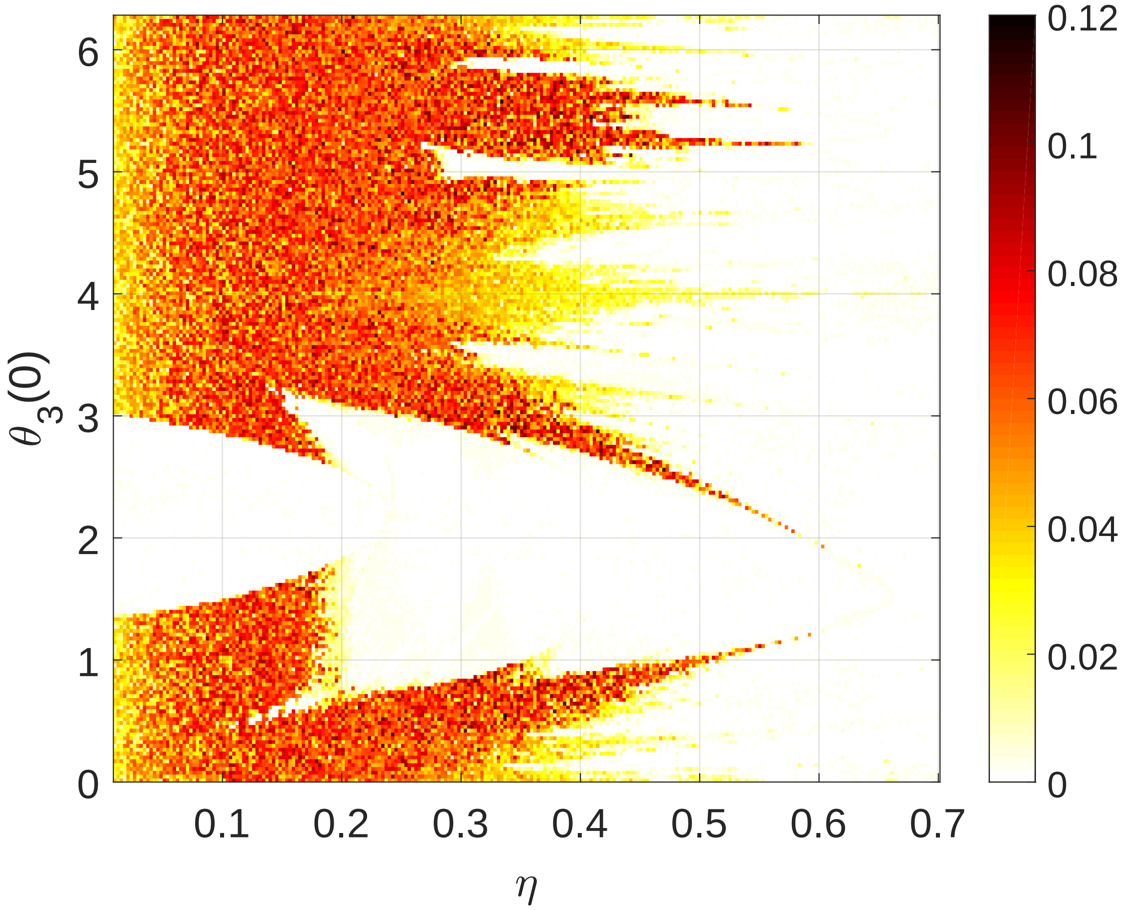

Figure 7: Maximal Lyapunov exponent for solutions starting with $\theta_1(0) = 0$, $\theta_2(0) = 4$ and $\theta_3(0)$ given by the value shown. Chaotic solutions have positive Lyapunov exponent. Parameters: $N = 3, n = 2, \kappa = -0.75$.

III. RESULTS FOR NETWORKS OF 4 NEURONS

We now move on to study networks of 4 neurons, described by (1)-(2) with $N = 4$. Rather than systematically searching through phase space we randomly and independently chose the initial values of the θ_i from $[0, 2\pi]$ and determine the maximal Lyapunov exponent for that solution. Doing this 2000 times at each of a number of discrete values of κ we obtain the results in Fig. 11, which shows the *probability* that a random initial condition will have a specific maximal Lyapunov exponent.

If we remove the self-coupling the resulting network is described by

$$\frac{d\theta_i}{dt} = 1 - \cos\theta_i + (1 + \cos\theta_i)(\eta + \kappa I_i) \tag{14}$$

for $i = 1, 2, 3, 4$, where

$$I_i = \frac{a_n}{3} \sum_{\substack{j=1 \\ j\neq i}}^{4} (1 - \cos\theta_j)^n \tag{15}$$

and a_n is as in (3). Sweeping over the same parameter range as in Fig. 11 we obtain very similar results (not shown).

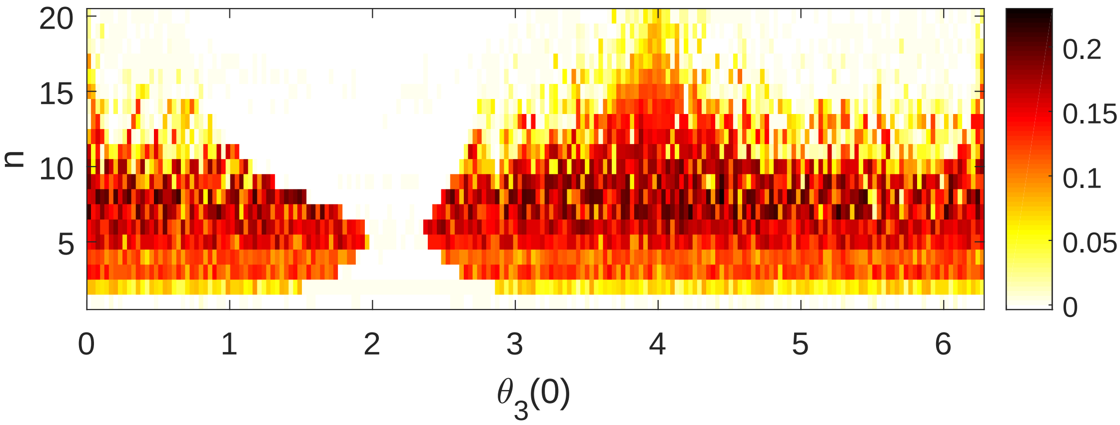

Figure 8: Maximal Lyapunov exponent for solutions starting with $\theta_1(0) = 0$, $\theta_2(0) = 4$ and $\theta_3(0)$ given by the value shown. Chaotic solutions have positive Lyapunov exponent. Parameters: $N = 3, \eta = 0.1, \kappa = -0.75$.

Now consider 4 neurons in a ring with self-coupling, with ordering by index. We have (14) but with

$$I_1 = a_n[(1 - \cos\theta_1)^n + (1 - \cos\theta_2)^n + (1 - \cos\theta_4)^n]/3 \quad (16)$$

$$I_2 = a_n[(1 - \cos\theta_2)^n + (1 - \cos\theta_3)^n + (1 - \cos\theta_1)^n]/3 \quad (17)$$

$$I_3 = a_n[(1 - \cos\theta_3)^n + (1 - \cos\theta_4)^n + (1 - \cos\theta_2)^n]/3 \quad (18)$$

$$I_4 = a_n[(1 - \cos\theta_4)^n + (1 - \cos\theta_1)^n + (1 - \cos\theta_3)^n]/3 \quad (19)$$

The results in Fig. 12. Keeping the ring structure but removing self-coupling gives similar results to Fig. 12 (not shown).

IV. DISCUSSION

We have investigated the robustness of chaotic behaviour in small networks of theta neurons with instantaneous coupling via current pulses. For a range of parameter values chaotic solutions coexist with quasiperiodic ones. This is consistent with the behaviour seen in other reversible systems [33, 34]. Note that the neurons do not have to be identical to observe chaotic behaviour.

If we break the system's reversibility by adding, for example, the unphysical term $0.02 \sin\theta_i$ to the RHS of (1), and repeat the calculations shown in Fig. 2, we find no initial conditions result in chaotic behaviour (not shown). This is consistent with previous results [9] which found that modifications such as dynamic synapses, gap junctional coupling or using conductance dynamics, all of which destroyed reversibility, also destroyed chaotic dynamics. Even though the theta neuron is the normal form of a saddle-node on an invariant circle bifurcation, its reversibility may not be shared by other neuron models also undergoing this bifurcation, but instead be an artifact of the reduction to normal form.

We have made no attempt to determine the origin of the chaotic behaviour seen, nor the transitions from quasiperiodic to chaotic dynamics as parameters are varied. In dissipative dynamical systems chaos may arise from a Shilnikov bifurcation [36], for example, but the systems studied here are reversible rather than dissipative. The role of chaos in neuroscience continues to be debated [37] but the main message here is that even very small networks of simple neurons can show surprisingly complex behaviour, although this is due to their nongeneric structure (reversibility, in this case). Thus, simpler models may not always have simpler behaviour.

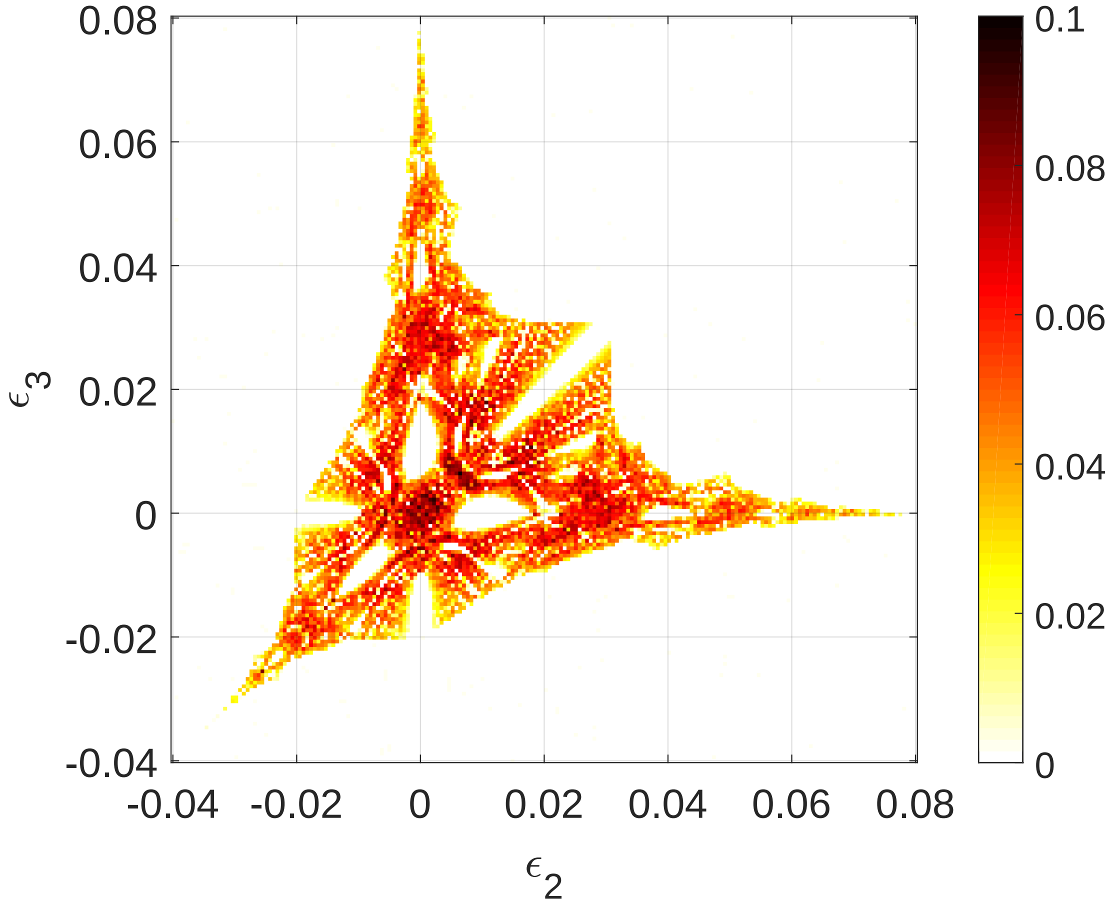

Figure 9: Maximal Lyapunov exponent for solutions starting with $\theta_1(0) = 0$, $\theta_2(0) = 4$ and $\theta_3(0) = 5$. Chaotic solutions have positive Lyapunov exponent. We have $(\eta_1, \eta_2, \eta_3) = (0.1, 0.1 + \epsilon_2, 0.1 + \epsilon_3)$ Parameters: $N = 3, n = 2, \kappa = -0.75$.

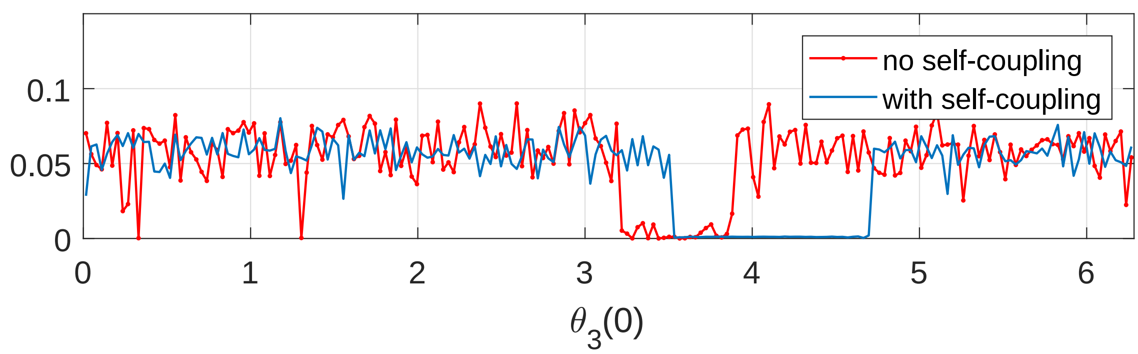

Figure 10: Maximal Lyapunov exponent for solutions starting with $\theta_1(0) = 0$, $\theta_2(0) = 2$ and $\theta_3(0)$ as shown. Blue solid line: the network (1)-(2), i.e. this is a vertical "slice" though Fig. 2 at $\theta_2(0) = 2$. Red dots and line: the network (10)-(11) (no self-coupling). We see that removing the self-coupling does not destroy the chaotic behaviour. Parameters: $N = 3, n = 2, \kappa = -0.75, \eta = 0.1$.

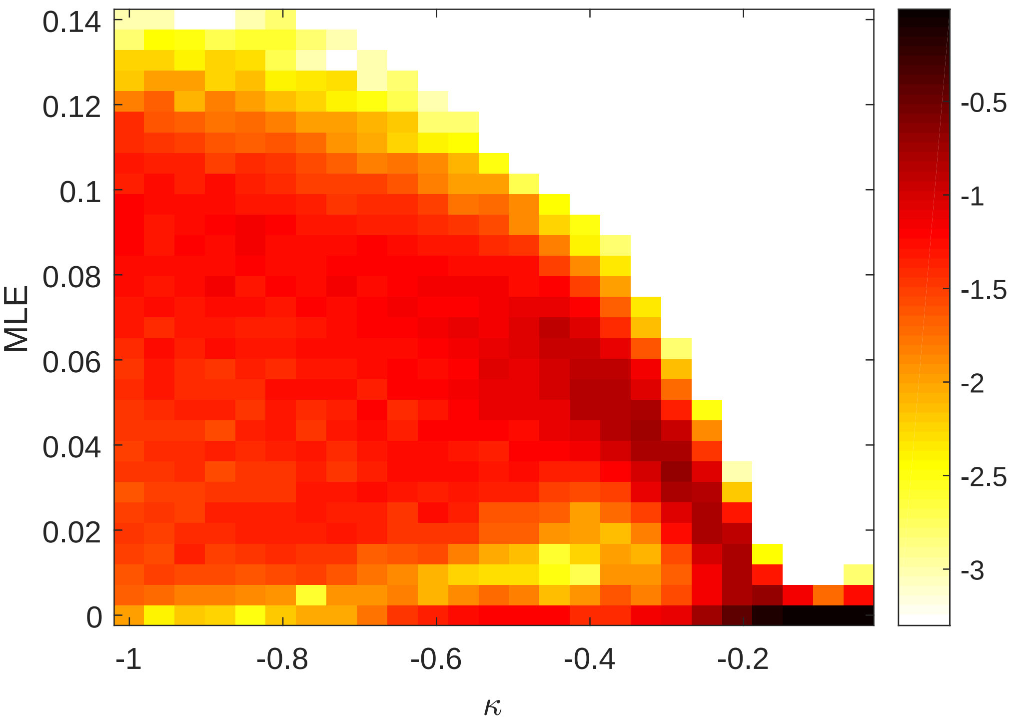

Figure 11: Probability of a randomly chosen initial condition having the maximal Lyapunov exponent (MLE) equal to the given value, as a function of κ. Log to the base 10 of the probability is shown, with white corresponding to low probability and black to high probability. (Bins with no entries are ignored.) This is an all-to-all coupled network. For a range of values of κ, many initial conditions result in chaotic solutions. Parameters: $N = 4, n = 2, \eta = 0.1$.

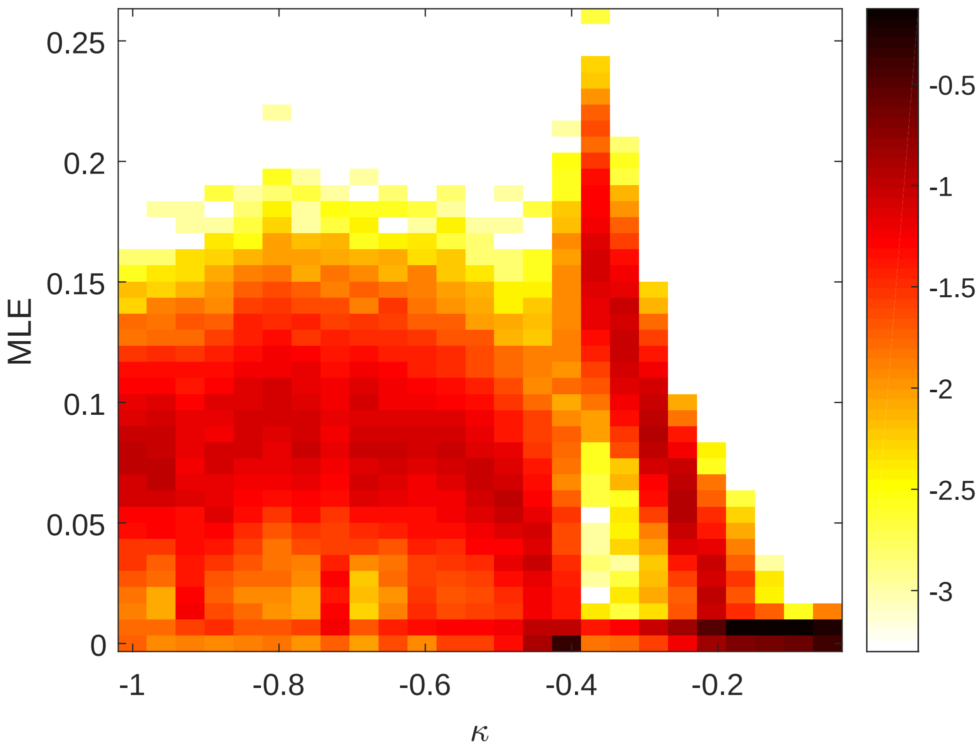

Figure 12: Probability of a randomly chosen initial condition having the maximal Lyapunov exponent (MLE) equal to the given value, as a function of κ. Log to the base 10 of the probability is shown, with white corresponding to low probability and black to high probability. (Bins with no entries are ignored.) This is a ring network with self-coupling described by (14) and (16)-(19). For a range of values of κ, many initial conditions result in chaotic solutions. Parameters: $N = 4, n = 2, \eta = 0.1$.

V. APPENDIX

We have a network described by

$$\frac{d\theta_i}{dt} = 1 - \cos\theta_i + (1+\cos\theta_i)(\eta + \kappa I) \tag{20}$$

where I is given by (8). Note that when a neuron fires it has no influence on itself as $1 + \cos\theta = 0$ at firing. Using the transformation [25]

$$\tan(\phi/2) = \frac{\tan(\theta/2)}{\sqrt{\eta}} \tag{21}$$

we have

$$\frac{d\phi_i}{dt} = 2\sqrt{\eta} + \frac{\kappa I}{\sqrt{\eta}}(1+\cos\phi_i) \tag{22}$$

The advantage of this formulation is that between firing times $I = 0$ and the ϕ_i increase at a constant speed. Suppose that t_{s-1} and t_s are two successive firing times of any of the neurons. Then

$$\phi_i(t_s) = \phi_i(t_{s-1}) + 2\sqrt{\eta}(t_s - t_{s-1}) \tag{23}$$

When any neuron fires we can use results from the theory of differential equations with state-dependent impulsive forcing [38] to derive the update rule

$$\phi_i(t_s^+) = 2\tan^{-1}\left[\tan\left(\frac{\phi_i(t_s^-)}{2}\right) + \frac{\pi\kappa}{N\sqrt{\eta}}\right] \equiv U[\phi_i(t_s^-)] \tag{24}$$

Given the last firing time t_{s-1} and the states of the neurons at that time, the next firing time is

$$t_s = t_{s-1} + \min_i\left[\frac{\pi - \phi_i(t_{s-1})}{2\sqrt{\eta}}\right] \tag{25}$$

Since the neurons have identical drive in the absence of coupling, the next neuron to fire will be the one with the largest phase after the last firing event. The mapping from one firing event at t_{s-1} to the one at t_s is

$$\phi_i(t_s) = f(\phi_i(t_{s-1})) = U[\phi_i(t_{s-1}) + 2\sqrt{\eta}(t_s - t_{s-1})] \tag{26}$$

for $i = 1, 2 \ldots N$. If neuron j caused the firing event, we set $\phi_j(t_s) = -\pi$.

The Jacobian of the map (26), $D(t_s)$, can be calculated analytically [25]. The ith diagonal entry of $D(t_s)$, $i = 1, 2 \ldots N$, is $d_i(t_s)$, where

$$d_i(t_s) = \frac{\left[\tan\left(\frac{\phi_i(t_s^-)}{2}\right)\right]^2 + 1}{\left[\tan\left(\frac{\phi_i(t_s^-)}{2}\right) + \frac{\pi\kappa}{N\sqrt{\eta}}\right]^2 + 1} \tag{27}$$

Suppose that neuron j is the one involved in firing at time t_s. Then the jth diagonal entry, from (27), is equal to 1. The ith entry in the jth column of $D(t_s)$ is $1 - d_i(t_s)$ and all other entries not mentioned above are zero. The largest Lyapunov exponent of a solution found by mapping (26) can be determined from the growth in the norm of solutions of the linear map

$$x(t_s) = D(t_s)x(t_{s-1}) \tag{28}$$

where $x \in \mathbb{R}^N$ and the initial value of x is chosen randomly.

[1] C. Geisler, N. Brunel, and X.-J. Wang, Journal of neurophysiology **94**, 4344 (2005).
[2] C. Börgers and N. Kopell, Neural computation **17**, 557 (2005).

[3] C. Laing and C. Chow, Neural Comput. **13**, 1473 (2001).
[4] E. Marder and D. Bucher, Current biology **11**, R986 (2001).
[5] J. Wojcik, J. Schwabedal, R. Clewley, and A. L. Shilnikov, PloS one **9**, e92918 (2014).
[6] P. Ashwin, S. Coombes, and R. Nicks, The Journal of Mathematical Neuroscience **6**, 2 (2016).
[7] M. Golubitsky, I. Stewart, P.-L. Buono, and J. Collins, Nature **401**, 693 (1999).
[8] M. Golubitsky, I. Stewart, and D. G. Schaeffer, *Singularities and groups in bifurcation theory*, vol. 51 (Springer-Verlag, 1985).
[9] C. R. Laing, The Journal of Mathematical Neuroscience **8**, 4 (2018).
[10] S. Watanabe and S. Strogatz, Phys. Rev. Lett. **70**, 2391 (1993).
[11] S. Watanabe and S. Strogatz, Physica D **74**, 197 (1994).
[12] P. Ashwin, Nonlinearity **3**, 603 (1990).
[13] G. Ermentrout and D. Terman, *Mathematical Foundations of Neuroscience*, vol. 35 (Springer Verlag, 2010).
[14] S. Strogatz, Physica D **143**, 1 (2000).
[15] J. Acebrón, L. Bonilla, C. Pérez Vicente, F. Ritort, and R. Spigler, Rev. Mod. Phys. **77**, 137 (2005).
[16] C. Bick, M. Timme, D. Paulikat, D. Rathlev, and P. Ashwin, Phys. Rev. Lett. **107**, 244101 (2011).
[17] O. V. Popovych, Y. L. Maistrenko, and P. A. Tass, Phys. Rev. E **71**, 065201 (2005).
[18] C. Bick, P. Ashwin, and A. Rodrigues, Chaos: An Interdisciplinary Journal of Nonlinear Science **26**, 094814 (2016).
[19] C. Bick, M. Panaggio, and E. Martens, arXiv preprint arXiv:1802.05481 (2018).
[20] C. R. Laing, Chaos **22**, 043104 (2012).
[21] M. Wolfrum, O. E. Omel'chenko, S. Yanchuk, and Y. L. Maistrenko, Chaos **21**, 013112 (2011).
[22] M. Wolfrum and E. Omel'chenko, Physical Review E **84**, 015201 (2011).
[23] B. Ermentrout, Neural computation **8**, 979 (1996).
[24] G. B. Ermentrout and N. Kopell, SIAM Journal on Applied Mathematics **46**, 233 (1986).
[25] M. Monteforte and F. Wolf, Physical review letters **105**, 268104 (2010).
[26] P. So, T. B. Luke, and E. Barreto, Physica D: Nonlinear Phenomena **267**, 16 (2014).
[27] D. Pazó and E. Montbrió, Physical review letters **116**, 238101 (2016).
[28] S. Luccioli and A. Politi, Phys. Rev. Lett. **105**, 158104 (2010), URL `https://link.aps.org/doi/10.1103/PhysRevLett.105.158104`.
[29] S. Jahnke, R.-M. Memmesheimer, and M. Timme, Physical Review Letters **100**, 048102 (2008).
[30] R. Zillmer, N. Brunel, and D. Hansel, Physical Review E **79**, 031909 (2009).
[31] B. Ermentrout, Scholarpedia **3**, 1398 (2008), revision #122128.
[32] T. B. Luke, E. Barreto, and P. So, Neural computation **25**, 3207 (2013).
[33] J. A. Roberts and G. R. W. Quispel, Physics Reports **216**, 63 (1992).
[34] A. Politi, G. Oppo, and R. Badii, Physical Review A **33**, 4055 (1986).
[35] H. Nakao, Contemporary Physics **57**, 188 (2016).
[36] L. P. Shilnikov and A. Shilnikov, Scholarpedia **2**, 1891 (2007), revision #153014.
[37] S. Coombes, SIAM Journal on Applied Dynamical Systems **7**, 1101 (2008).
[38] A. J. Catllá, D. G. Schaeffer, T. P. Witelski, E. E. Monson, and A. L. Lin, SIAM review **50**, 553 (2008).